Supporting Information

Slot-Die Coated Ternary Organic Photovoltaics for Indoor Light Recycling

Mahmoud E. Farahat, [†] *Audrey Laventure,* [†] *Michael A. Anderson,* [§] *Mathieu Mainville,* [‡] *Francesco Tintori,* [†] *Mario Leclerc,* [‡] *Erin L. Ratcliff*,* [§Δ#] *Gregory C. Welch*,* [†]

†Department of Chemistry, University of Calgary, 2500 University Drive N.W., Calgary, Alberta, Canada T2N 1N4.

§Department of Materials Science and Engineering, University of Arizona, Tucson, AZ 85721, USA.

‡Department of Chemistry, Université Laval, Quebec City, Qc, Canada, G1V 0A6

ΔDepartment of Chemical and Environmental Engineering, University of Arizona, Tucson, AZ 85721, USA.

#Department of Chemistry and Biochemistry, University of Arizona, Tucson, AZ 85721, USA.

Table of contents

Table S1 Photovoltaic parameters of OPV devices using the binary systems (FBT:$PC_{61}BM$) and (FBT:PDI) with different additives *p*-anisaldehyde (AA) and diphenyl ether (DPE) used for solution processing (1% v/v in *o*-xylene).

Condition	V_{oc} (V)	J_{sc} (mA/cm^2)	FF (%)	PCE (%)
FBT: $PC_{61}BM$ (1:1.5) with DPE	0.73	10.9	60	4.8
FBT: $PC_{61}BM$ (1:1.5) with AA	0.76	12.5	73	7.0
FBT: PDI (1:1.5), with DPE	1.01	9.2	47	4.3
FBT: PDI (1:1.5), with AA	1.01	7.5	41	3.1

Device architecture: glass/ITO/ZnO/active layer/MoO_X/Ag

Devices spin coated from *o*-xylene containing 1% AA or 1% DPE as additive, 20 mg/mL total concentration and (1:1.5) weight ratio.

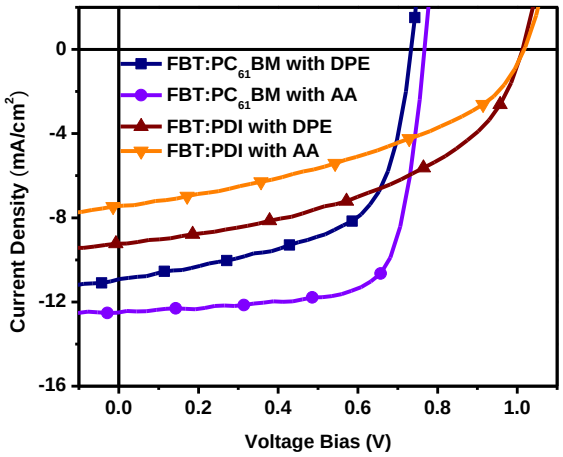

Figure S1 *J–V* curves of OPV devices using the binary systems (FBT:$PC_{61}BM$) and (FBT:PDI) with different additives *p*-anisaldehyde (AA) and diphenyl ether (DPE) used for solution processing (1% v/v in *o*-xylene).

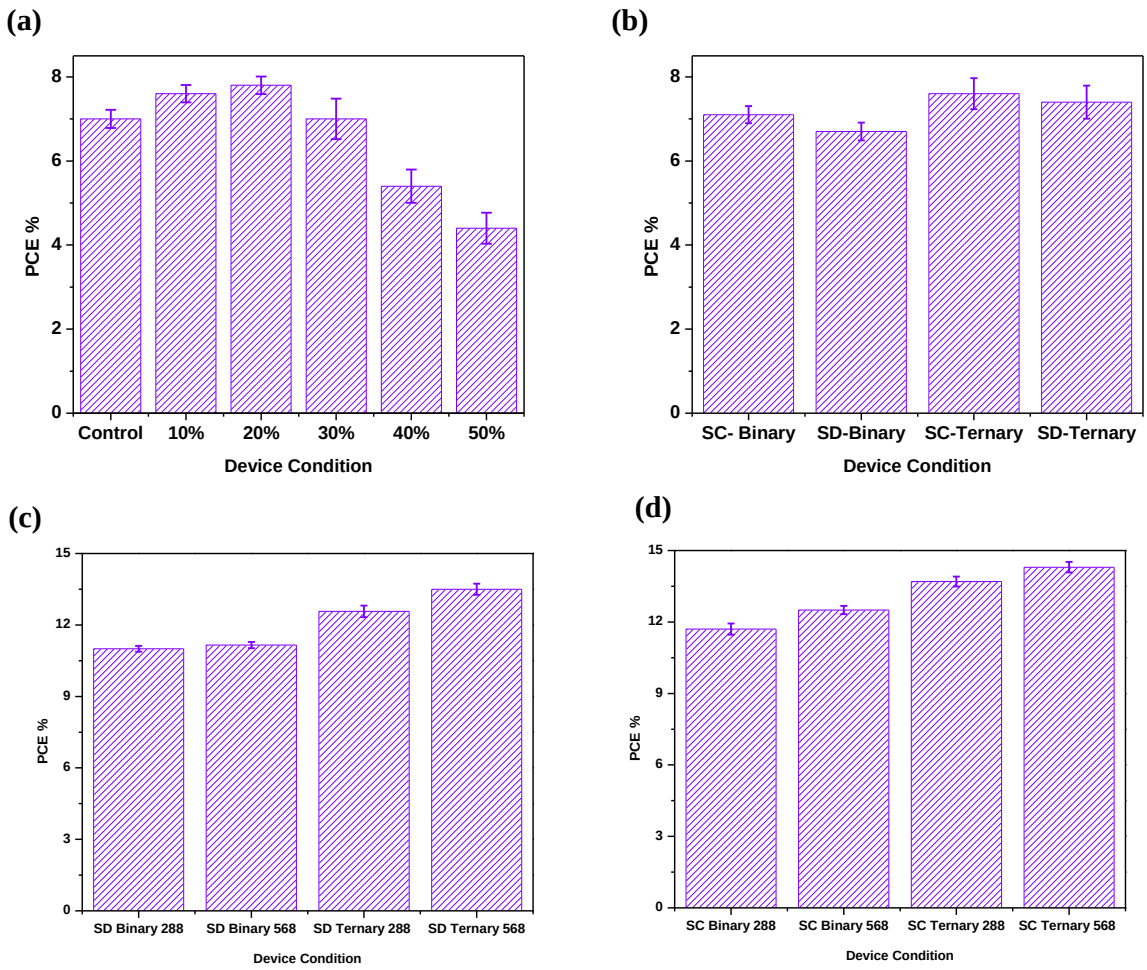

Figure S2 Standard deviation of the values reported in Table 1 (a), Table 2 (b) and Table 3 (c, d)

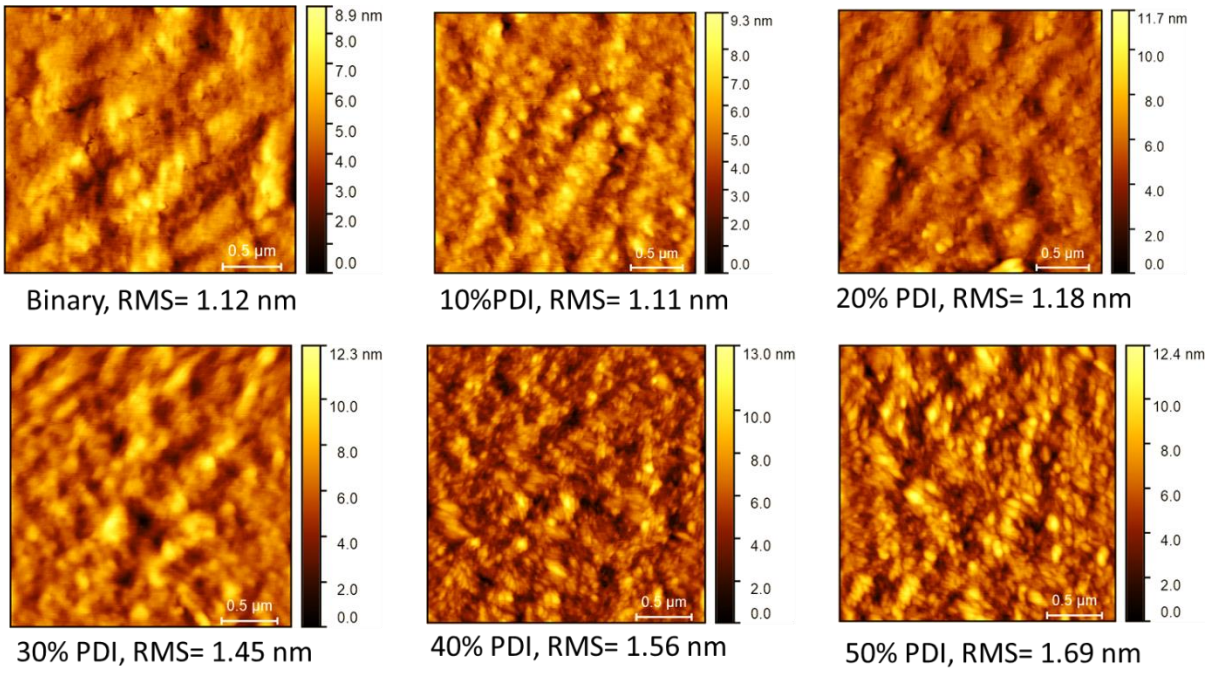

Figure S3 AFM height image of binary vs ternary films with different PDI component as a third component (spin coated).

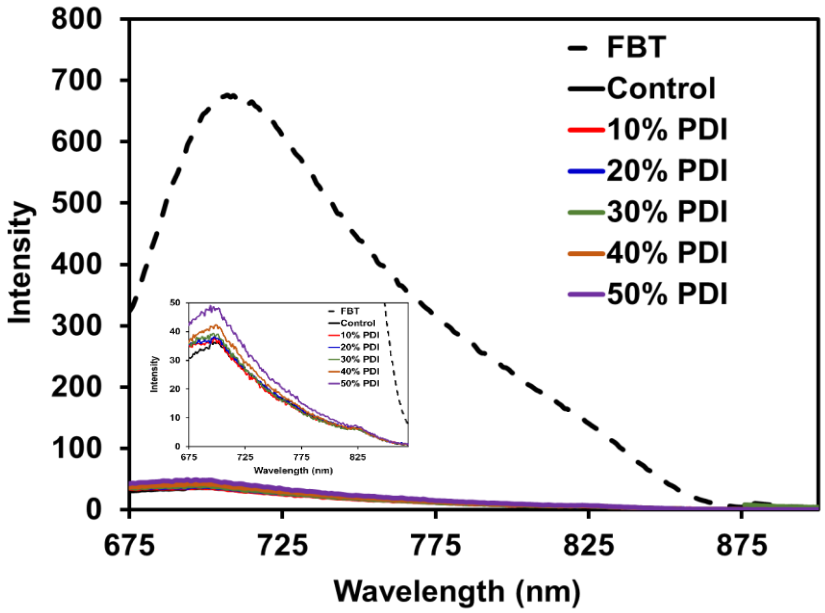

Figure S4 PL spectra of binary vs ternary films with different PDI component as a third component (spin coated).

Table S2 Photovoltaic parameters of OPV devices using spin coated (SC) binary and ternary active layers under 1 sun illumination. (a) FBT prepared as reported in reference (1) and (b) FBT provided by Brilliant Matters.

Condition	V_{oc} (V)	J_{sc} (μA/cm^2)	FF%	PCE%
ZnO				
Binary [a]	0.76 (0.76)	13 (12.7)	72 (72)	7.1 (6.9)
Ternary [a]	0.83 (0.83)	13.2 (12.9)	69 (69)	7.6 (7.4)
Binary [b]	0.76 (0.76)	12.5 (12.4)	73 (73)	7.0 (7.0)
Ternary [b]	0.86 (0.86)	13.4 (13.2)	68 (68)	7.9 (7.8)
ZnO/PEIE				
Binary [a]	0.77 (0.76)	13.1 (12.4)	74 (73)	7.4 (7)
Ternary [a]	0.85 (0.85)	13.4 (12.8)	73 (72)	8.3 (7.9)
Binary [b]	0.79 (0.78)	12.74 (12.6)	74 (72)	7.4 (7.1)
Ternary [b]	0.86 (0.86)	13.2 (12.9)	69 (69)	7.9 (7.6)

Device architecture: glass/ITO/ ZnO or (ZnO/PEIE)/active layer/MoO_X/Ag

Devices spin coated from *o*-xylene containing 1% AA additive, 20 mg/mL total concentration and (1:1.5) D:A_1:A_2 ratio (D: FBT, A_1: $PC_{61}BM$, and A_2: PDI).

The values of the best device are reported, while the values in the parentheses stand for the average PCEs from over 15 devices with 0.14 cm^2 active area.

[a] FBT prepared as reported in reference (1) [1].

[b] FBT provided by Brilliant Matters

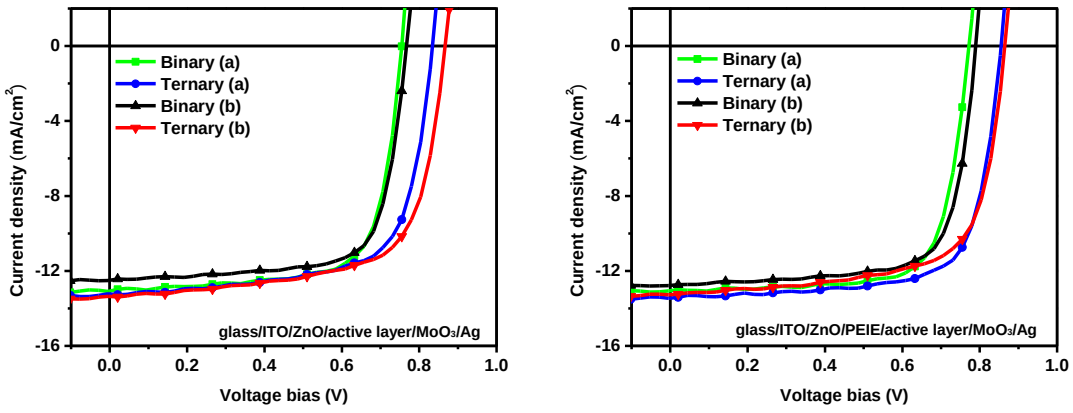

Figure S5 *J–V* curves of OPV devices using spin coated (SC) binary and ternary active layers under 1 sun illumination. (a) FBT prepared as reported in reference (1) and (b) FBT provided by Brilliant Matters.

Power input (P_{in}) measurements and calculations: The P_{in} was measured using a Newport Si-photodiode (818-SL/DB, 1cm^2 area) connected to an Ossila XTralien X200 source measure unit. The Si-photodiode was positioned at three different distance from the LED light bulb, corresponding to the three distances at which the OPV devices were positioned upon their testing. The current produced by the Si-photodiode were recorded at both 2700 K and 6500 K LED illumination (shown in Figure S6, as exemplified in Figure S7A).

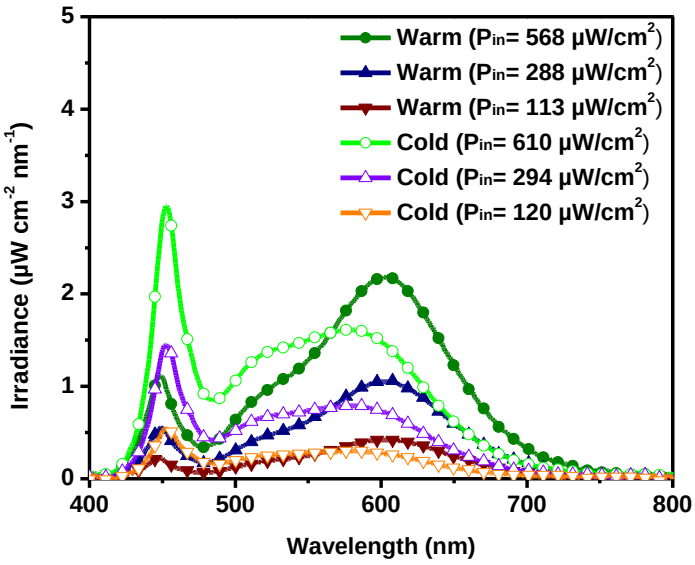

Figure S6 Different emission spectra of a Coidak bulb used for indoor light illumination. Model No: FUT105, Power: 12W, Voltage: AC86~265V 50~60 Hz, Color Temperature: 2700-6500K.

A) **B)**

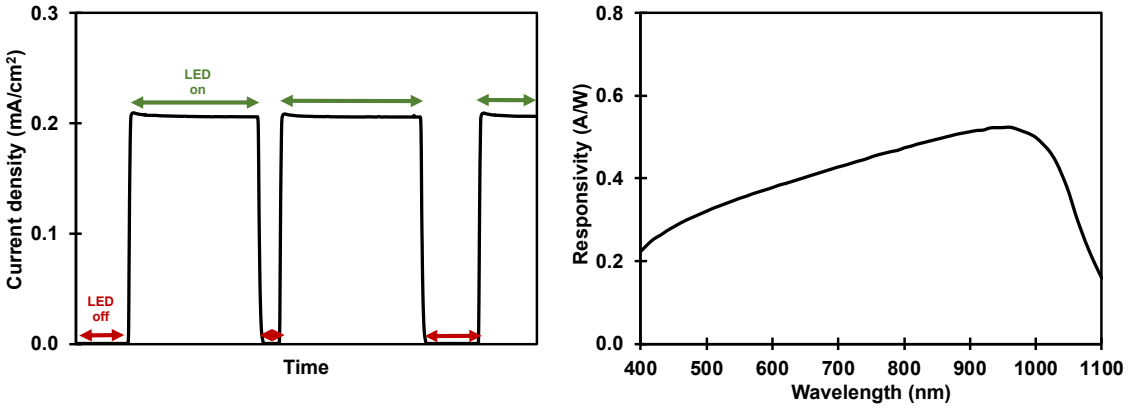

Figure S7 Si-photodiode A) current density response under a 2700 K LED illumination (distance A, ca. X lux) and B) responsivity.

Table S3 Current density response ($J_{measured}$, mA/cm^2) of the Si-photodiode under the different LED illumination used for the OPV testing.

	$J_{measured}$ at Distance A (mA/cm^2)	**$J_{measured}$ at Distance B** (mA/cm^2)	**$J_{measured}$ at Distance C** (mA/cm^2)
2700 K	0.208	0.105	0.041
6500 K	0.209	0.101	0.041

The P_{in} was then calculated using Equation S1.

$$P_{in} = K \times \int \Phi_{LED,\,normalized} = \frac{J_{measured}}{J_{calculated}} \times \int \Phi_{normalized} = \frac{J_{measured}}{\int \Phi_{LED,\,normalized} \times R_{photodiode}} \times \int \Phi_{LED,\,normalized}$$

Equation S1

Where $J_{measured}$ corresponds to the current density response of the Si-photodiode (values reported in Table S3); Φ_{LED} is the irradiance spectra of the LED (Figure S6) and $R_{photodiode}$ (Figure S7 B) is the responsivity of the Si-photodiode.

The calculated P_{in} values are reported in Table S4.

Table S4 P_{in} values (in μW/cm^2) calculated according to Equation S1.

	Distance A	**Distance B**	**Distance C**
2700 K	568	288	113
6500 K	610	294	120

Illuminance measurements and calculations. The illuminance (*I*) measurements were measured using a commercial digital luxmeter (Dr Meter). The values are reported in Table S5. The illuminance at which the OPV devices were tested can also be calculated using the Si-photodiode response, according to Equation S2 and considering that the lm/m^2 unit corresponds to the lux unit.

$$I = 683\ \frac{lm}{W} \times \mathrm{K} \times \int \Phi_{\mathrm{LED,\ normalized\ @\ 555\ nm}} \times V \qquad \textbf{Equation S2}$$

$$= 683\ \frac{lm}{W} \times \frac{J_{measured}}{J_{calculated}} \times \int \Phi_{LED,normalized\ @\ 555\ nm} \times V$$

$$= 683\ \frac{lm}{W} \times \frac{\mathrm{J_{measured}}}{\int \Phi_{\mathrm{LED,\ normalized}} \times \mathrm{R_{photodiode}}} \times \int \Phi_{\mathrm{LED,\ normalized\ @\ 555\ nm}} \times V$$

Where *I* corresponds to the illuminance values and *V* is the photopic response (Figure S8). Since the photopic response function has a maximum at 555 nm, the 683 lm/W factor is used at the luminous efficiency and could be responsible of the discrepancy between the $I_{measured}$ and $I_{calculated}$ that are reported in Table S5.

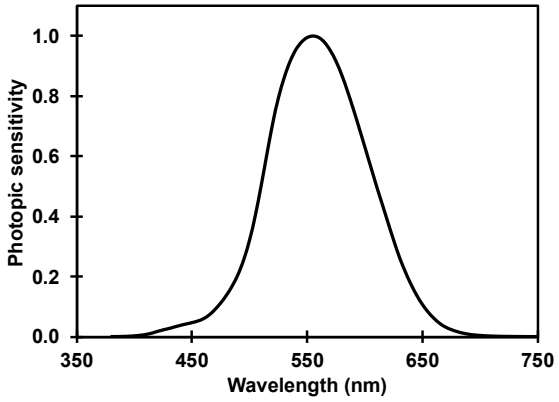

Figure S8 Photopic response function.

Table S5 Illuminance values ($I_{measured}$ using a digital luxmeter and $I_{calculated}$ according to Equation S2) reported in lux.

	Distance A	**Distance B**	**Distance C**
2700 K			
$I_{measured}$	1750-1800	870-900	350-380
$I_{calculated}$	1410	714	282
6500 K			
$I_{measured}$	1900-1950	930-970	380-400
$I_{calculated}$	1230	597	243

Integrated current calculation from EQE for indoor OPVs

According to recent reports in Nature Energy,[2] Advanced Materials,[3] and ACS AMI,[4] for a photovoltaic cell, the EQE curve is independent of the emission spectrum of the light source. EQE curves measured from the AM 1.5G condition can be used to get the integral current density (J_{cal}) for indoor measurements. J_{cal} from EQE is expected to be consistent with the J_{SC} from J–V measurement for the same device. The J_{cal} is calculated by the following equation:

$$Jcal = q.\int_0^{\infty} N\,(\lambda).EQE(\lambda)\,d\lambda$$

Where N (λ) is the photon flux spectrum which is the light photon numbers per nanometer per square centimeter through the spectrometer and can be obtained by the following equation:

$$N\,(\lambda) = E\,(\lambda)\,.q\lambda/hc$$

Where E (λ) is the light power spectrum (irradiance), q is the elementary charge, λ is the wavelength, h corresponds to the Planck constant and c is the lightspeed.

To confirm that the EQE under AM 1.5G condition can be used for indoor, we calculated the J_{cal} according to the above equations for the spin coated ternary devices and found that the current is 165.5 μA/cm^2 which is matching with the measured J_{sc} of 167.4 μA/cm^2 under warm white LED (2000 lux: input power is 568 μW/cm^2).

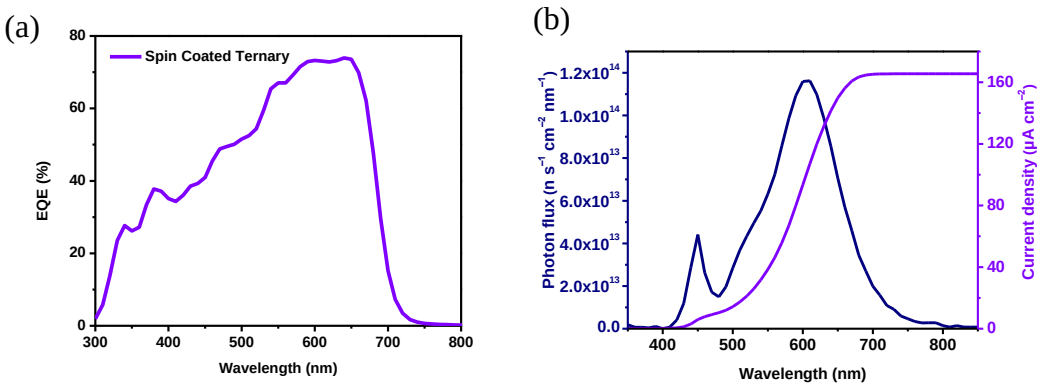

Figure S9 (a) EQE spectrum of the OPV devices with spin coated ternary active layers (optimized FBT batch)[1] and (b) photon flux and integrated current density spectrum over the warm white LED (2000 lux: input power is 568 μW/cm^2) for OPV devices with spin-coated ternary active layers.

Table S6 Photovoltaic parameters of OPV devices with spin coated (SC) binary and ternary active layers under different warm indoor light illumination.

P_{in} (μW/cm^2)	V_{oc} (V)	J_{sc} (μA/cm^2)	FF (%)	PCE (%)	P_{out} (μW/cm^2)
Binary (ZnO/PEIE)					
113	0.58 (0.58)	33 (32.7)	68 (66)	11.5 (11.1)	13.0 (12.5)
288	0.61(0.61)	84.3 (83.3)	68 (67)	12.1 (11.8)	35.0 (34)
568	0.64 (0.64)	157.8 (157.8)	70 (68)	12.4 (12.1)	70.7 (68.7)
Ternary (ZnO/PEIE)					
113	0.65 (0.65)	33.5 (33.4)	65 (64)	12.5 (12.3)	14.2 (13.9)
288	0.68 (0.68)	83.4 (83)	67 (66)	13.2 (12.9)	38.0 (37.2)
568	0.72 (0.71)	157.4 (159.6)	70 (68)	14.0 (13.6)	79.3 (77.1)

Device architecture: glass/ITO/ ZnO or (ZnO/PEIE)/active layer/MoO_X/Ag

Devices spin coated from *o*-xylene containing 1% AA additive, 20 mg/mL total concentration and (1:1.5) D:A_1:A_2 ratio (D: FBT, A_1: $PC_{61}BM$, and A_2: PDI). **FBT polymer provided by Brilliant Matters.**

The values of the best device are reported, while the values in the parentheses stand for the average PCEs from over 15 devices with 0.14 cm^2 active area.

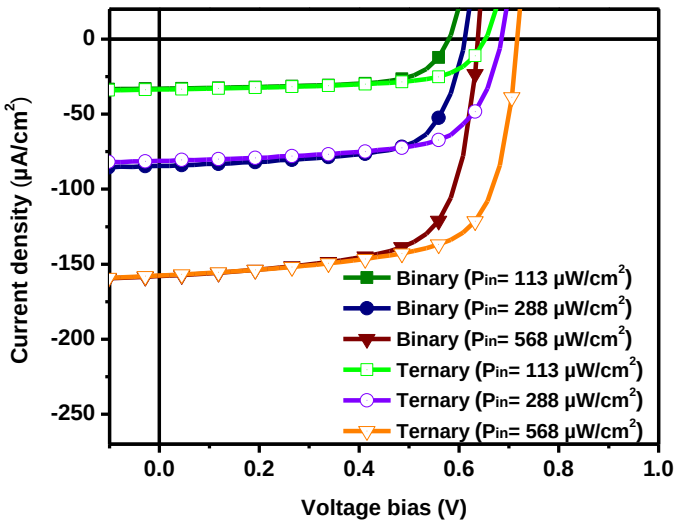

Figure S10 *J–V* curves of OPV devices with spin coated (SC) binary and ternary active layers under different warm indoor light illumination.

Table S7 Photovoltaic parameters of OPV devices with spin coated (SC) binary and ternary active layers under different warm indoor light illumination.

P_{in} (μW/cm^2)	V_{oc} (V)	J_{sc} (μA/cm^2)	FF (%)	PCE (%)	P_{out} (μW/cm^2)
Binary (ZnO)					
113	0.55 (0.55)	34.5 (34.5)	68 (67)	11.4 (11.3)	12.9 (12.7)
288	0.58	86.2	68	11.8	34
568	0.61 (0.61)	170.4 (169.3)	70 (69)	12.8 (12.5)	72.8 (71.3)
Ternary (ZnO)					
113	0.62 (0.62)	34.5 (33.5)	67 (68)	12.7 (12.5)	14.3 (14.1)
288	0.65	88.4	66	13.2	37.9
568	0.68 (0.68)	161.1 (163)	70 (68)	13.5 (13.3)	76.7 (75.4)

Device architecture: glass/ITO/ ZnO/active layer/MoO_X/Ag

Devices spin coated from *o*-xylene containing 1% AA additive, 20 mg/mL total concentration and (1:1.5) D:A_1:A_2 ratio (D: FBT, A_1: $PC_{61}BM$, and A_2: PDI). **FBT polymer prepared as reported in reference (1).**

The values of the best device are reported, while the values in the parentheses stand for the average PCEs from over 15 devices with 0.14 cm^2 active area.

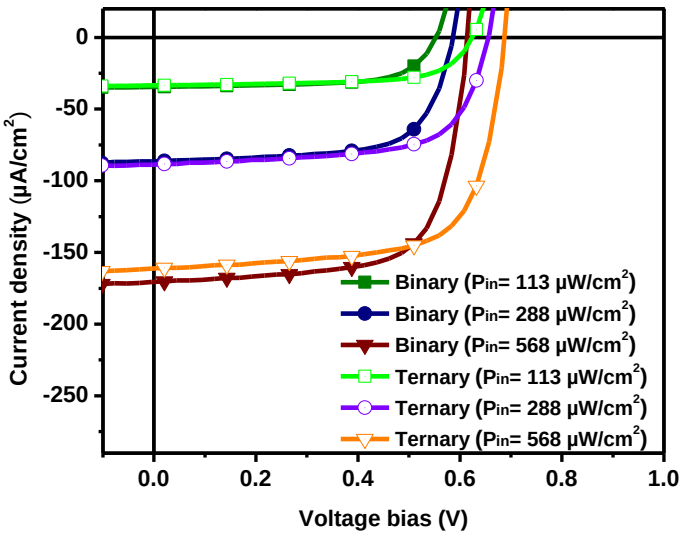

Figure S11 *J–V* curves of OPV devices with spin coated (SC) binary and ternary active layers under different warm indoor light illumination.

Table S8 Photovoltaic parameters of OPV devices with spin coated (SC) binary and ternary active layers under different warm indoor light illumination.

P_{in} (μW/cm^2)	V_{oc} (V)	J_{sc} (μA/cm^2)	FF (%)	PCE (%)	P_{out} (μW/cm^2)
Binary (ZnO/PEIE)					
113	0.57 (0.57)	35.1 (33.2)	70 (69)	12.4 (11.6)	14.0 (13.1)
288	0.61 (0.60)	86.2 (81)	70 (69)	12.8 (11.6)	36.8 (33.5)
568	0.63 (0.63)	162.4 (154)	73 (73)	13.2 (12.5)	74.7 (70.8)
Ternary (ZnO/PEIE)					
113	0.66 (0.65)	35.9 (34.4)	69 (68)	14.4 (13.5)	16.3 (15.2)
288	0.69 (0.68)	87.3 (83.5)	70 (69)	14.6 (13.6)	42.2 (39.2)
568	0.72 (0.72)	167.4 (159)	73 (71)	15.5 (14.3)	88.0 (81.3)

Device architecture: glass/ITO/ZnO/PEIE/active layer/MoO_X/Ag

Devices spin coated from *o*-xylene containing 1% AA additive, 20 mg/mL total concentration and (1:1.5) D:A_1:A_2 ratio (D: FBT, A_1: $PC_{61}BM$, and A_2: PDI). **FBT polymer prepared as reported in reference (1).**

The values of the best device are reported, while the values in the parentheses stand for the average PCEs from over 15 devices with 0.14 cm^2 active area.

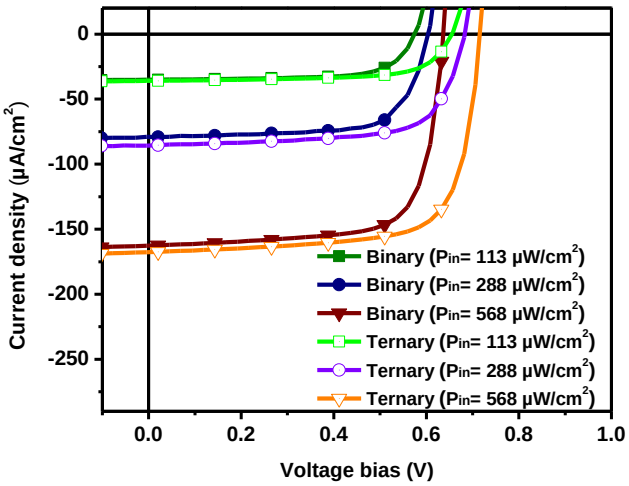

Figure S12 *J–V* curves of OPV devices with spin coated (SC) binary and ternary active layers under different warm indoor light illumination.

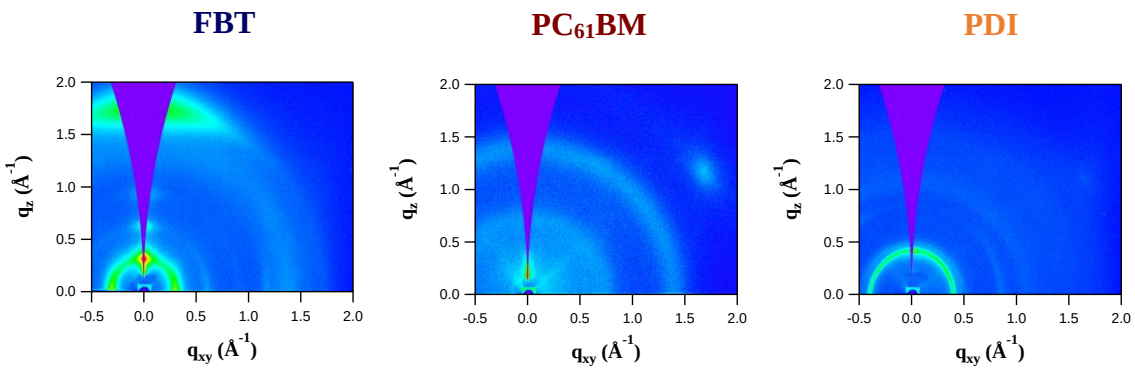

Figure S13 GIWAXS 2D detector images for FBT, $PC_{61}BM$, and PDI.

FBT

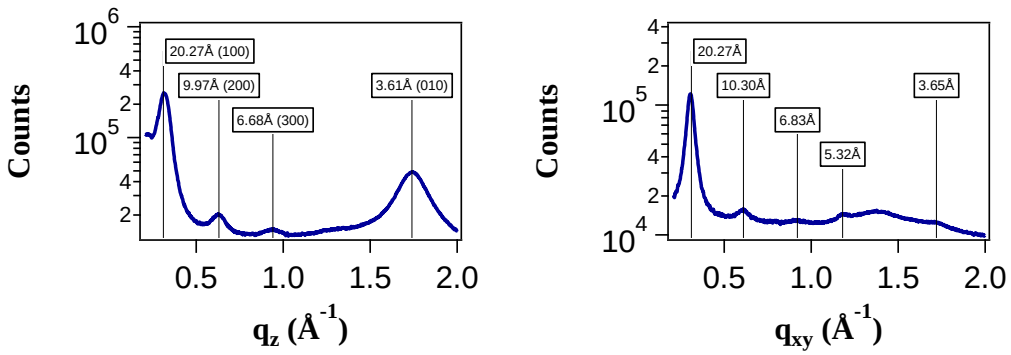

$PC_{61}BM$

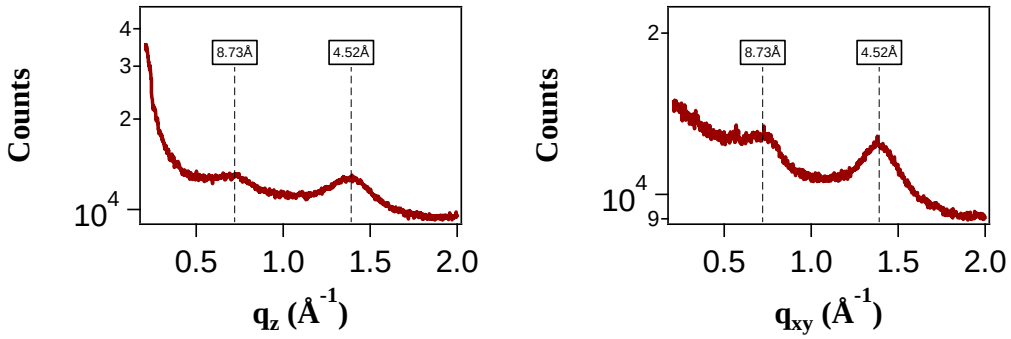

PDI

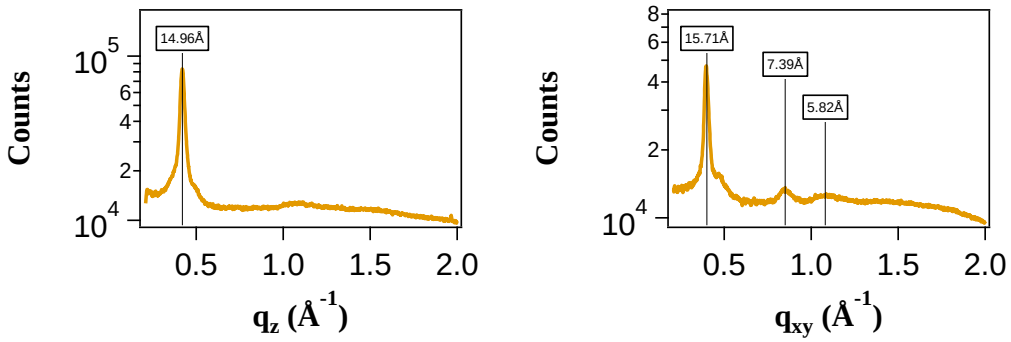

Binary SD

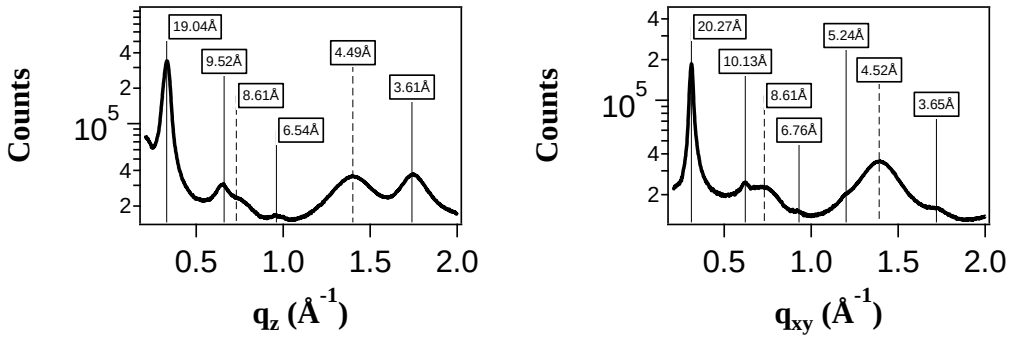

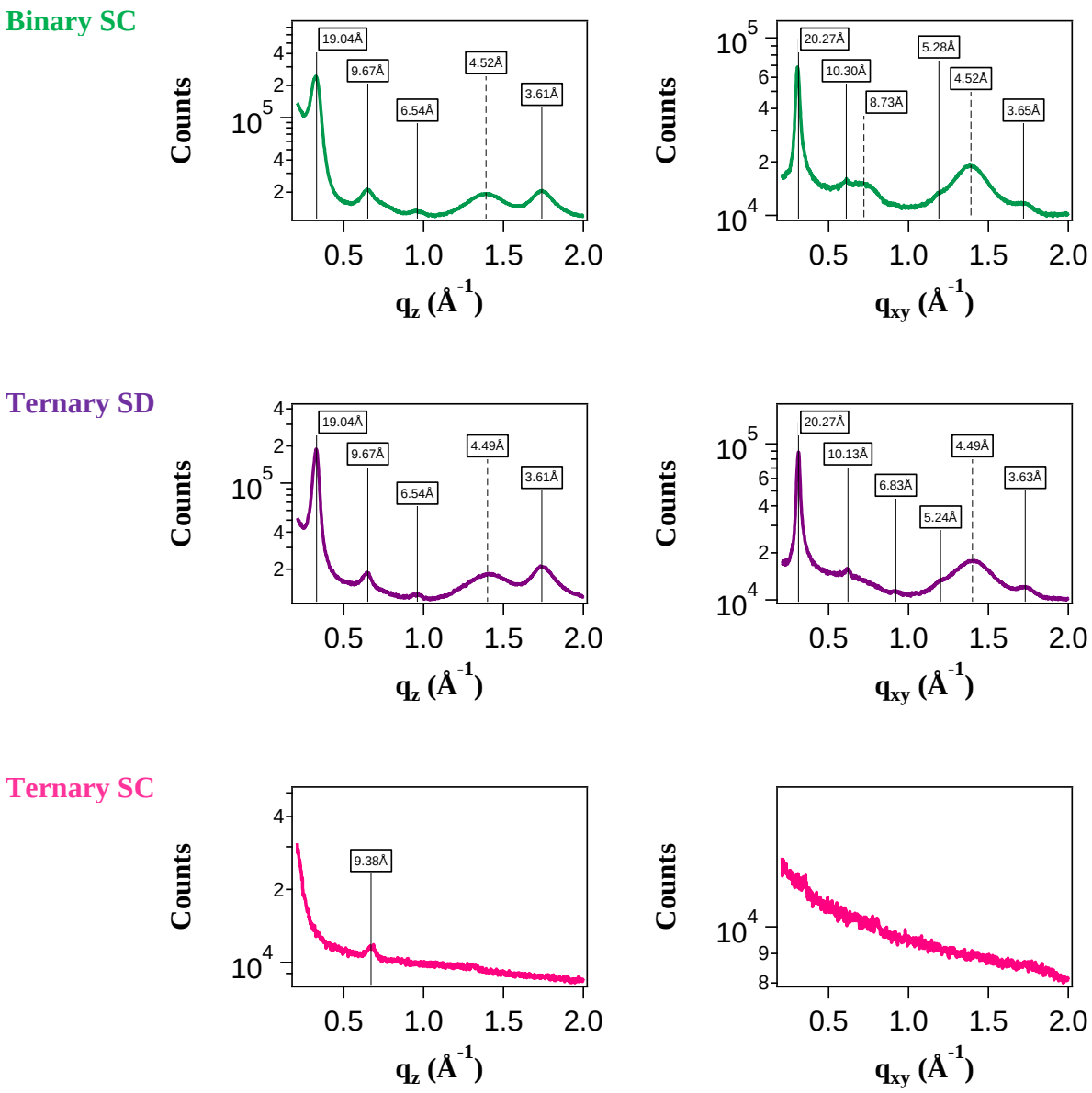

Figure S14 GIWAXS 1D plots with cake slices in the q_z (out-of-plane) and q_{xy} (in-plane).

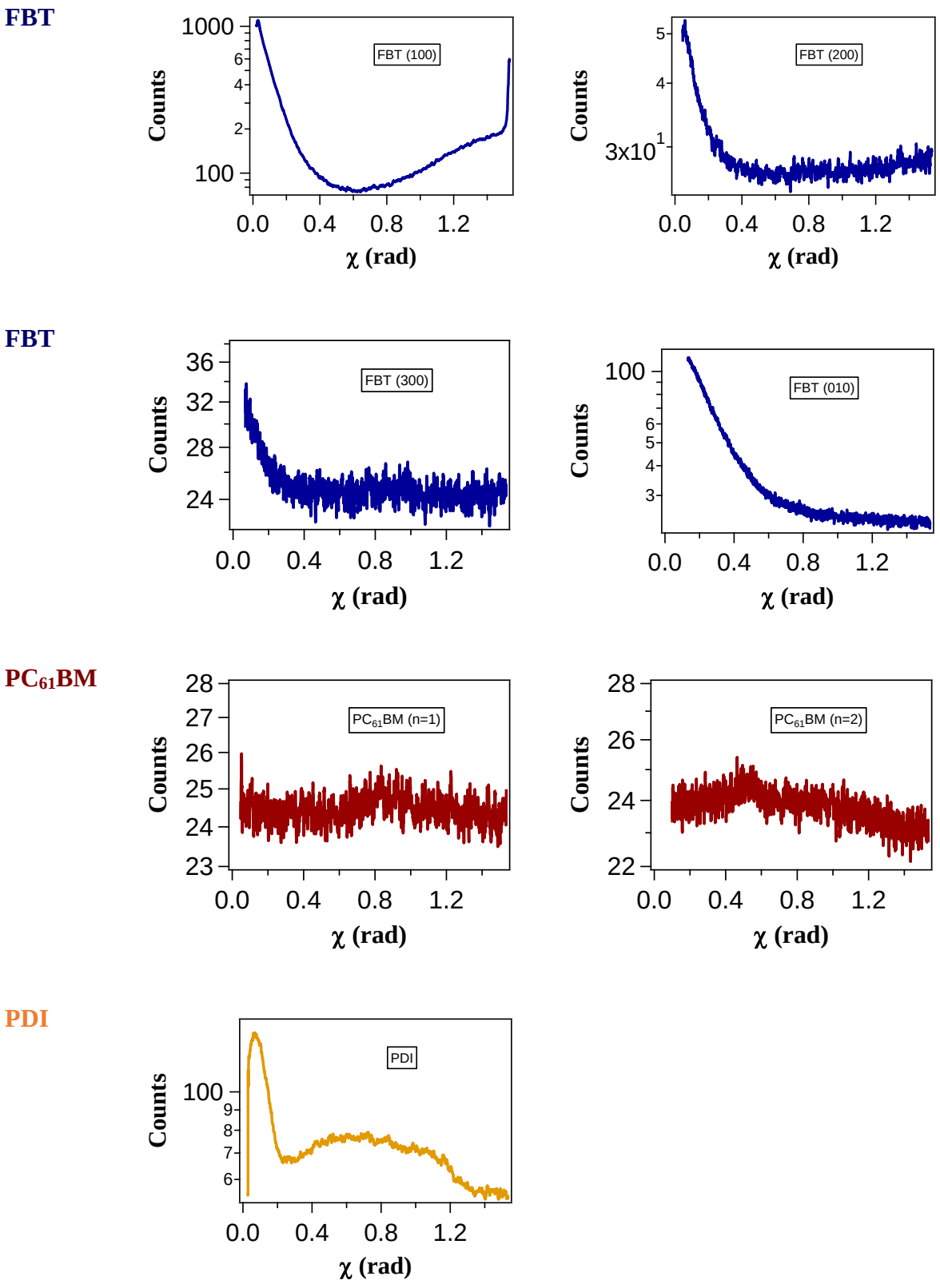

Figure S15 GIWAXS chi plots as intensity vs. angle for the prominent 1D peaks.

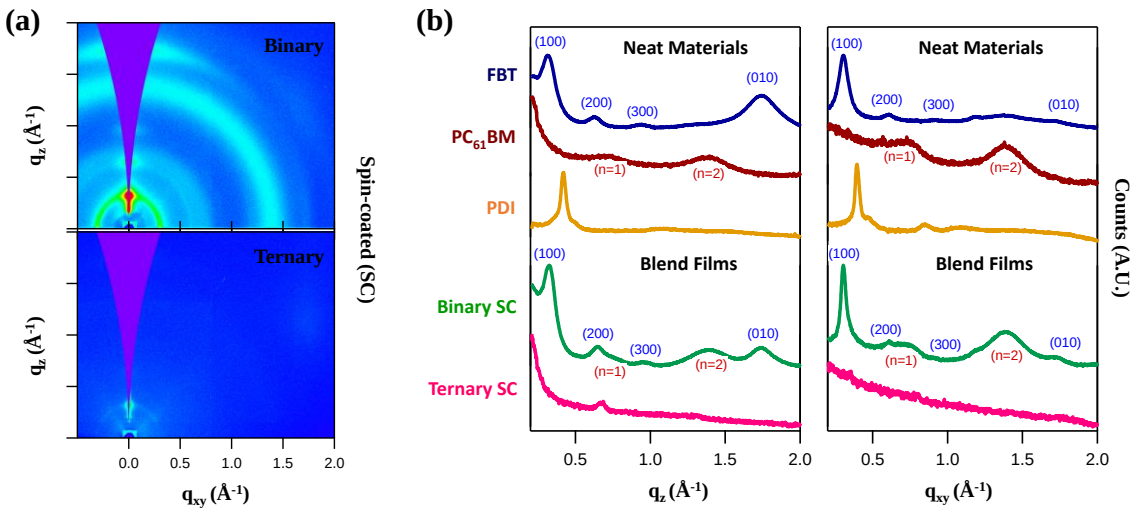

Figure S16 GIWAXS (a) 2-dimensional intensity vs. q-space images for the spin-coated blend films and (b) one-dimensional intensity vs. q_z-space (left) and q_{xy}-space (right).

Table S9 Intermolecular spacings in Angstroms of the semi-crystalline regions in neat and spin-coated blend films from the peaks of q_z-space in Figure S16 (b).

	d-spacing (Å)						
Sample	**FBT**				**$PC_{61}BM$**		**PDI**
	(100)	**(200)**	**(300)**	**(010)**	**(n=1)**	**(n=2)**	
FBT	20.27	9.97	6.68	3.61	—	—	—
$PC_{61}BM$	—	—	—	—	8.73	4.52	—
PDI	—	—	—	—	—	—	14.96
Binary SC	19.04	9.67	6.54	3.61	—	4.52	—
Ternary SC	—	9.38	—	—	—	—	—

Table S10 Contact angle measurements of using binary and ternary blend inks on different substrates.

Substrate	Average contact angle (°)
Bare Si (Binary Ink)	8.6
Bare Si (Ternary Ink)	13.0
Si/ZnO/PEIE (Binary Ink)	21.4
Si/ZnO/PEIE (Ternary Ink)	12.0
ITO/ZnO/PEIE (Binary Ink)	9.4
ITO/ZnO/PEIE (Ternary Ink)	10.6

Contact angles measured using Ossila Contact Angle Geniometer (product code: L2004A1)

1- The binary ink: FBT:$PC_{61}BM$ (1:1.5, 20 mg/mL) in *o*-xylene with 1% (v/v) *p*-anisaldehyde (AA) as solvent additive.

2- The ternary ink: FBT:$PC_{61}BM$:PDI (1:1.2:0.3, 20 mg/mL) in *o*-xylene with 1% (v/v) *p*-anisaldehyde (AA) as solvent additive.

Inks were drop-cast onto the substrate and the droplet angle measured.

Table S11 Photovoltaic parameters of OPV devices under warm low light intensity (2000 lux) with and without light soaking.

Condition	Pin (μW/cm^2)	V_{oc} (V)	J_{sc} (μA/cm^2)	FF%	PCE%	Pout (μW/cm^2)
W/O light soaking (LS)	568	0.71	133	40	6.7	38
LS with UV filter	568	0.71	166	44	9.1	52
LS- W/O UV filter	568	0.71	169	70	14.8	84

Device architecture: glass/ITO/ ZnO/PEIE/active layer/MoO_X/Ag

Devices spin coated from *o*-xylene containing 1% AA additive, 20 mg/mL total concentration and (1:1.5) D:A_1:A_2 ratio (D: FBT (optimized batch), A_1: $PC_{61}BM$, and A_2: PDI).

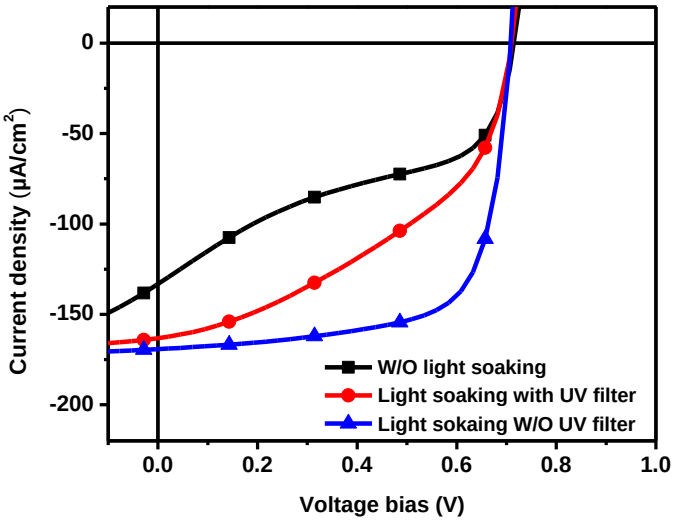

Figure S17 *J–V* curves of OPV devices under warm low light intensity (2000 lux) with and without light soaking.

Table S12 Photovoltaic parameters of OPV devices with slot-die (SD) coated binary and ternary active layers using different electron transporting layers under indoor warm light illumination (2000 lux).

P_{in} (μW/cm^2)	V_{oc} (V)	J_{sc} (μA/cm^2)	FF (%)	PCE (%)	P_{out} (μW/cm^2)
Binary (ZnO/PEIE), light soaking required					
568 (w)	0.63 (0.63)	154 (147)	70 (68)	12.0 (11.1)	68 (63)
Binary (ZnO), light soaking required					
568 (w)	0.61 (0.61)	164.2 (155.3)	68.0 (65)	12.0 (10.8)	68.1 (61.6)
Binary (PEIE), NO light soaking required					
568 (w)	0.57 (0.55)	163 (160.5)	63 (58)	10.3 (9.0)	58.5 (51.2)

Device architecture: glass/ITO/ ZnO or (ZnO/PEIE) or PEIE/active layer/MoO_X/Ag

Devices slot-die coated from *o*-xylene containing 1% AA additive, 20 mg/mL total concentration and (1:1.5).

The values of the best device are reported, while the values in the parentheses stand for the average PCEs from over 15 devices with 0.14 cm^2 active area.

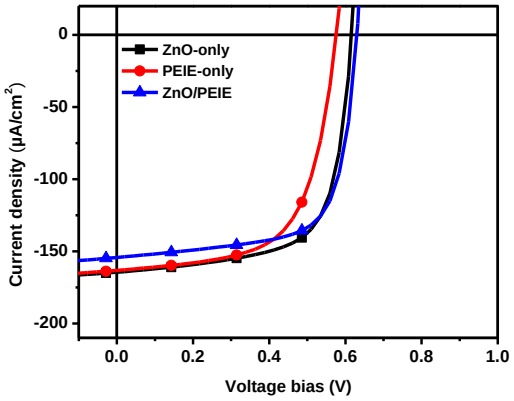

Figure S18 *J–V* curves of OPV devices with slot-die (SD) coated binary and ternary active layers using different electron transporting layers under indoor warm light illumination (2000 lux).

Stability tests according to ISOS

According to the International Summit on Organic Photovoltaic Stability (ISOS) protocols,[5,6] there are 5 stability tests to evaluate the OPVs stability performance:

1- Dark (ISOS-D-1-3)
2- Outdoor (ISOS-O-1-3)
3- Laboratory weathering testing (ISOS-L-1-3)
4- Thermal cycling (ISOS-T-1-3)
5- Solar-thermal-humidity Cycling (ISOS-LT-1-3)

We performed the stability tests according to the stability testing protocol ISOS-D-1 and ISOS-T-1

		ISOS-D-1 (Shelf)	ISOS-T-1 (thermal cycling)
Test setup	Light source	None (Dark)	None (Dark)
	Load	Open circuit	Open circuit
	Storage temperature	Ambient	65/85 ℃ by cycling on/off hot plate
	Storage relative humidity (R.H.)	Ambient and inert	Inert (N_2 filled glovebox)[7]
	Characterization light source	Solar simulator	Solar simulator

In a recent review[8] the authors mentioned in the Miscellaneous Stability Measurements section that:

1- In the thermal stability measurement, there are two categories of test conditions: 1) under high-temperature condition above 100 °C, and 2) under low-temperature condition below 100 °C.

2- In the storage stability test, there are three widely used conditions: 1) stored in the air without encapsulation; 2) stored in the air with encapsulation and; 3) stored in an inert atmosphere.

Here in our work and according to the previous references, we performed three stability tests:

1- Storage in inert conditions of unencapsulated devices under dark for 500 hours.
2- Storage in ambient conditions of unencapsulated devices under dark for 300 hours.
3- Thermal stability at 80 °C at inert conditions under dark for 300 hours.

REFERENCES

(1) Mainville, M.; Tremblay, V.; Fenniri, M. Z.; Laventure, A.; Farahat, M. E.; Ambrose, R.; Welch, G. C.; Hill, I. G.; Leclerc, M. Water Compatible Direct (Hetero)Arylation Polymerization of PPDT2FBT: A Pathway Towards Large-Scale Production of Organic Solar Cells. *Asian J. Org. Chem.* **2020**, *9*, 1–9.

(2) Cui, Y.; Wang, Y.; Bergqvist, J.; Yao, H.; Xu, Y.; Gao, B.; Yang, C.; Zhang, S.; Inganäs, O.; Gao, F.; Hou, J. Wide-Gap Non-Fullerene Acceptor Enabling High-Performance Organic Photovoltaic Cells for Indoor Applications. *Nat. Energy* **2019**, *4* (9), 768–775.

(3) Cui, Y.; Yao, H.; Zhang, T.; Hong, L.; Gao, B.; Xian, K.; Qin, J.; Hou, J. 1 Cm2 Organic Photovoltaic Cells for Indoor Application with over 20% Efficiency. *Adv. Mater.* **2019**, *31* (42), 1904512.

(4) Cui, Y.; Hong, L.; Hou, J. Organic Photovoltaic Cells for Indoor Applications: Opportunities and Challenges. *ACS Appl. Mater. Interfaces* **2020** (doi.org/10.1021/acsami.0c10444)

(5) Reese, M. O.; Gevorgyan, S. A.; Jørgensen, M.; Bundgaard, E.; Kurtz, S. R.; Ginley, D. S.; Olson, D. C.; Lloyd, M. T.; Morvillo, P.; Katz, E. A.; Elschner, A.; Haillant, O.; Currier, T. R.; Shrotriya, V.; Hermenau, M.; Riede, M.; R. Kirov, K.; Trimmel, G.; Rath, T.; Inganäs, O.; Zhang, F.; Andersson, M.; Tvingstedt, K.; Lira-Cantu, M.; Laird, D.; McGuiness, C.; Gowrisanker, S. (Jimmy); Pannone, M.; Xiao, M.; Hauch, J.; Steim, R.; DeLongchamp, D. M.; Rösch, R.; Hoppe, H.; Espinosa, N.; Urbina, A.; Yaman-Uzunoglu, G.; Bonekamp, J.-B.; van Breemen, A. J. J. M.; Girotto, C.; Voroshazi, E.; Krebs, F. C. Consensus Stability Testing Protocols for Organic Photovoltaic Materials and Devices. *Sol. Energy Mater. Sol. Cells* **2011**, *95* (5), 1253–1267.

(6) Jørgensen, M.; Norrman, K.; Gevorgyan, S. A.; Tromholt, T.; Andreasen, B.; Krebs, F. C. Stability of Polymer Solar Cells. *Adv. Mater.* **2012**, *24* (5), 580–612.

(7) Nguyen, T. L.; Choi, H.; Ko, S.-J.; Uddin, M. A.; Walker, B.; Yum, S.; Jeong, J.-E.; Yun, M. H.; Shin, T. J.; Hwang, S.; Kim, J. Y.; Woo, H. Y. Semi-Crystalline Photovoltaic Polymers with Efficiency Exceeding 9% in a ∼300 Nm Thick Conventional Single-Cell Device. *Energy Environ. Sci.* **2014**, *7* (9), 3040–3051.

(8) Duan, L.; Uddin, A. Progress in Stability of Organic Solar Cells. *Adv. Sci.* **2020**, *7* (11), 1903259.